DOI: 10.1021/cg901353e

CRYSTAL GROWTH & DESIGN Article

2010, Vol. 10 1307–1311

# Two Thermostable Three-Dimensional Homochiral Metal−Organic Polymers with Quartz Topology

Li-Li Liang, Shi-Bin Ren, Jun Zhang, Yi-Zhi Li, Hong-Bin Du,* and Xiao-Zeng You

*State Key Laboratory of Coordination Chemistry, Nanjing National Laboratory of Microstructures, School of Chemistry and Chemical Engineering, Nanjing University, Nanjing 210093, P. R. China*

*Received October 30, 2009*

**ABSTRACT:** Two new homochiral metal−organic coordination polymers, $M_2$(TPOM)(D-Cam)$_2$($H_2O$)$_2$ (M = Zn for **1**, Cd for **2**, D-$H_2$cam = D-camphoric acid, TPOM = tetrakis(4-pyridyloxymethylene)methane) have been prepared under solvothermal conditions and characterized by single crystal X-ray structure analyses, thermogravimetric analyses, circular dichroism, second-order nonlinear optical (NLO), and photoluminescent measurements. Compounds **1** and **2** are isostructural and crystallize in the chiral space group $P2_12_12$ (No. 18). In **1**, Zn(II) is tetrahedrally coordinated, while Cd(II) in **2** is six-coordinated. Both possess a three-dimensional (3D) framework with a 4-connected node. Tetrahedral quadridentate linker TPOM connects four M(II) ions through its four peripheral pyridyl groups to form a wavelike two-dimensional (2D) sheet $[M_2(TPOM)]_n$. The chiral bidentate D-$H_2$cam ligand connects two M(II) ions to form a homochiral left-handed one-dimensional helical chain $[M(D\text{-cam})]_n$. The homochiral helical chains interweave the 2D wavelike sheets via sharing the metal sites to form a 3D homochiral framework with 2-fold interpenetrating quartz ($6^48^2$) topology. Both **1** and **2** are NLO-active materials and exhibit relatively high thermal stabilities.

## Introduction

Chiral porous materials are of great importance for their tremendous potential applications in enantioselective separations, asymmetric catalysis, etc.[1−3] The availability of inexpensive and robust chiral porous materials is for a long time desirable. However, the synthesis of chiral porous materials, particularly zeolite molecular sieves, is one of the most challenging issues in synthetic chemistry.[1] Even though a few, either naturally occurring or synthesized, chiral porous inorganic materials are known, the preparation of enantiopure, thermostable zeolites has been proven to be very difficult. In recent years, there has been an intensive focus on the synthesis of porous metal−organic frameworks (MOFs).[3−5] Novel MOFs with specific structures and functional properties could be prepared by combining the metal ions with functional multidentate organic ligands of a certain coordination geometry. Through careful design of chiral ligands, one can judiciously prepare chiral porous MOFs. Compared to inorganic four-connected porous materials, the synthesis of chiral MOFs has met with some success, and a number of chiral MOFs have been synthesized thus far.[3−9] Nonetheless, MOFs are usually less thermostable compared to inorganic materials, which limits their applications. The rational design and construction of homochiral coordination polymers with good thermal stabilities remain a challenge.

Currently, the widely adopted approach to build chiral MOFs is to use predesigned chiral ligands. D-Camphoric acid is one of the well-known chiral construction materials due to its special "V" shape and its relatively low price since it can be easily prepared from the naturally rich D-camphor. A number of chiral and homochiral porous MOFs have been constructed using D-camphoric acid,[6−9] in several cases in the presence of auxiliary organic amines,[8,9] for example, linear or nonlinear bidentate bipyridines such as 4,4′-bipyridine,[8a−c] *trans*-1,2-bis(4-pyridyl)-ethylene,[8b−d] 4,4′-trimethylenedipyridine,[8e,f] etc. Tridentate 2,4,5-tri(4-pyridyl)-imidazole[9a] and tetradentate 1,2,4,5-tetra(4-pyridyl)benzene[9b] in combination with chiral D-camphorates have also been reported to construct chiral MOFs. But both ligands have planar geometry that limits the topology variety. We explored the coassembly of the tetrahedral quadridentate linker tetrakis(4-pyridyloxymethylene)methane (TPOM)[10] with D-camphoric acid and expected to build chiral zeolitic MOFs with the tetrahedral connecting node. Herein we report the synthesis of two new isostructural chiral materials $Zn_2$(TPOM)(D-Cam)$_2$($H_2O$)$_2$, **1**, and $Cd_2$(TPOM)(D-Cam)$_2$($H_2O$)$_2$, **2**, (D-$H_2$cam = D-camphoric acid) (Scheme 1). Compounds **1** and **2** were characterized by single crystal X-ray structure analyses, thermogravimetric, circular dichroism, second-order NLO, and photoluminescent analyses.

**Scheme 1. Synthesis of 1 and 2**

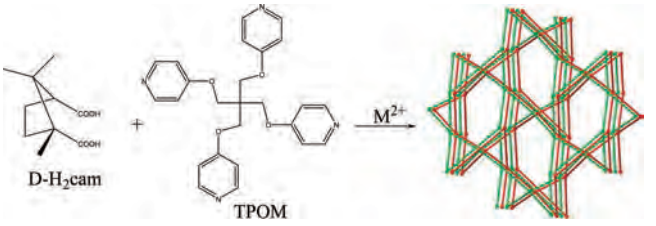


## Experimental Section

**General Procedures.** All chemicals were commercially available and used without further purification. The ligand TPOM was synthesized according to the literature method.[11] D-Camphoric acid was prepared from the oxidation of D-camphor.[12] Elemental analyses for C, H, and N were performed on a CHN-O-Rapid analyzer and an Elementar Vario MICRO analyzer. Powder X-ray diffraction (PXRD) patterns were collected in the $2\theta$ = 5−50° range with a

*To whom correspondence should be addressed. E-mail: hbdu@nju.edu.cn.



Published on Web 11/20/2009

**Table 1. Crystallographic Data Collection and Refinement Parameters for 1 and 2**

| | 1 | 2 |
|---|---|---|
| chemical formula | $C_{45}H_{56}N_4O_{14}Zn_2$ | $C_{45}H_{56}N_4O_{14}Cd_2$ |
| formula weight | 1007.68 | 1101.74 |
| crystal system | orthorhombic | orthorhombic |
| space group | $P2_12_12$ | $P2_12_12$ |
| $T$ (K) | 291(2) | 291(2) |
| wavelength (Å) | 0.71073 | 0.71073 |
| $a$ (Å) | 14.373(2) | 13.2749(9) |
| $b$ (Å) | 18.920(3) | 18.8649(13) |
| $c$ (Å) | 8.7804(13) | 9.7598(7) |
| $Z$ | 2 | 2 |
| $V$ (Å$^3$) | 2387.7(6) | 2444.1(3) |
| density (calculated g/cm$^3$) | 1.4015 | 1.4969 |
| abs coeff (mm$^{-1}$) | 1.073 | 0.937 |
| $F$(000) | 1052 | 1124 |
| crystal size (mm$^3$) | 0.18 × 0.16 × 0.16 | 0.26 × 0.22 × 0.20 |
| no. of reflections collected | 13073 | 13387 |
| no. of independent reflections /R(int) | 4693 | 4789 |
| no. of reflections observed ($I > 2\sigma(I)$) | 3690 | 4117 |
| GOF on $F^2$ | 1.043 | 1.094 |
| $R_1$, $wR_2$ ($I > 2\sigma(I)$)[a] | 0.0543, 0.1080 | 0.0513, 0.1168 |
| $R_1$, $wR_2$ (all data)[a] | 0.0655, 0.1104 | 0.0576, 0.1183 |
| largest diff peak and hole (e Å$^{-3}$) | 0.259, −0.484 | 0.585, −0.712 |

[a] $R_1 = \Sigma||F_o| - |F_c||/\Sigma|F_o|$, $wR_2 = [\Sigma w(F_o^2 - F_c^2)^2/\Sigma w(F_o^2)^2]^{1/2}$.

scan speed of 0.2 s/deg on a Bruker D8 diffractometer with Cu Kα ($\lambda$ = 1.542 Å) radiation equipped with a LynxEye detector at room temperature. Thermogravimetrical analyses (TGA) were performed in $N_2$ atmosphere (a flow rate of 100 mL min$^{-1}$) on a simultaneous SDT 2960 thermal analyzer from 25 °C up to 1000 °C, with a heating rate of 10 °C/min. The second-order nonlinear optical intensity was estimated by measuring a powder sample relative to urea. A pulsed Q-switched Nd:YAG laser at a wavelength of 1064 nm was used to generate a SHG signal. The backscattered SHG light was collected by a spherical concave mirror and passed through a filter that transmits only 532 nm radiation. The circular dichroism (CD) spectra of **1** and **2** were recorded at room temperature with a Jasco J-810(S) spectropolarimeter (KBr pellets). Luminescence spectra for the solid samples were recorded on an AMINCO Bowman Series2 fluorescence spectrophotometer.

**Single-Crystal X-ray Diffraction Analysis.** The suitable crystals of **1** and **2** with the dimensions 0.18 × 0.16 × 0.16 mm$^3$ for **1** and 0.26 × 0.22 × 0.20 mm$^3$ for **2** were selected for single crystal X-ray diffraction and the data were collected at 291 K on a Bruker Smart CCD diffractometer with a graphite-monochromatic Kα radiation ($\lambda$ = 0.71073 Å) from an enhanced optic X-ray tube. Data reductions and absorption corrections were performed using the SAINT and SADABS software packages, respectively. The structure was solved by direct methods and refined by full matrix least-squares methods on F2 using the SHELXS-97[13] and SHELXL-97 programs,[14] using atomic scattering factors for neutral atoms. Hydrogen atoms were placed in calculated positions and refined as riding atoms with a uniform value of $U_{iso}$. The crystallographic data and selected bond lengths and angles are listed in Tables 1 and 2, respectively.

**Synthesis of $Zn_2$(TPOM)(D-Cam)$_2$($H_2O$)$_2$ (1).** A solvothermal reaction of D-$H_2$Cam (0.0203 g, 0.1 mmol), TPOM (0.0446 g, 0.1 mmol), and $Zn(NO_3)_2 \cdot 6H_2O$ (0.0601 g, 0.2 mmol) in 4 mL of $H_2O$/EtOH (1:1 volume ratio) was performed at 100−120 °C for 2 days, and the mixture was then cooled to room temperature. The colorless rectangular crystals of **1** were obtained in 61% yield (based on D-$H_2$Cam). Elemental analyses calcd. (%) for **1**: C, 53.63: N, 5.56: H, 5.60. Found: C, 53.61; N, 5.54; H, 5.51.

**Synthesis of $Cd_2$(TPOM)(D-Cam)$_2$($H_2O$)$_2$ (2).** A solvothermal reaction of D-$H_2$Cam (0.0102 g, 0.05 mmol), TPOM (0.0224 g, 0.05 mmol), and $Cd(NO_3)_2 \cdot 4H_2O$ (0.0308 g, 0.1 mmol) in 2 mL of $H_2O$/EtOH (1:3 volume ratio) was performed at 120 °C for 2 days, and the mixture was then cooled to room temperature. The colorless cubic crystals of **2** were obtained in 37% yield (based on D-$H_2$Cam). Elemental analyses calcd. (%) for **2**: C, 49.06; N, 5.09; H, 5.12. Found: C, 49.08; N, 5.09; H, 5.07.

**Table 2. Selected Bond Lengths (Å) and Angles (deg) for 1 and 2[a]**

| | | | |
|---|---|---|---|
| | | **1** | |
| N1−Zn1 | 2.064(4) | O5$^{vi}$−Zn1−N1 | 129.57(15) |
| N2−Zn1 | 2.078(3) | O3−Zn1−N1 | 104.38(14) |
| O3−Zn1 | 1.960(3) | O5$^{vi}$−Zn1−N2 | 107.91(14) |
| O5−Zn1$^{v}$ | 1.942(3) | O3−Zn1−N2 | 97.18(13) |
| O5$^{vi}$−Zn1−O3 | 114.98(15) | N1−Zn1−N2 | 96.59(15) |
| | | **2** | |
| Cd1−N1 | 2.281(5) | N1−Cd1−O3$^{vi}$ | 105.37(16) |
| Cd1−O3$^{vi}$ | 2.320(4) | N1−Cd1−O2 | 152.27(15) |
| Cd1−O2 | 2.324(4) | O3$^{vi}$−Cd1−O2 | 102.02(15) |
| Cd1−O4$^{vi}$ | 2.326(4) | N1−Cd1−O4$^{vi}$ | 101.64(16) |
| Cd1−N2 | 2.332(5) | O3$^{vi}$−Cd1−O4$^{vi}$ | 55.79(15) |
| Cd1−O1 | 2.342(4) | O2−Cd1−O4$^{vi}$ | 90.09(16) |
| O3$^{vi}$−Cd1−O1 | 155.20(15) | N1−Cd1−N2 | 88.68(19) |
| O2−Cd1−O1 | 55.12(14) | O3$^{vi}$−Cd1−N2 | 93.07(16) |
| O4$^{vi}$−Cd1−O1 | 109.93(15) | O2−Cd1−N2 | 94.18(18) |
| N2−Cd1−O1 | 97.75(17) | O4$^{vi}$−Cd1−N2 | 148.71(18) |
| N1−Cd1−O1 | 97.16(15) | | |

[a] For **1**: (i) −0.5 + $x$, 1.5 − $y$, 3 − $z$; (ii) 0.5 + $x$, 1.5 − $y$, 3 − $z$; (iii) 0.5 − $x$, −0.5 + $y$, 3 − $z$; (iv) 1 − $x$, 1 − $y$, $z$; (v) 0.5 + $x$, 1.5 − $y$, 1 − $z$; (vi) −0.5 + $x$, 1.5 − $y$, 1 − $z$. For **2**: (i) 1.5 − $x$, −0.5 + $y$, 2 − $z$; (ii) 1 − $x$, 2 − $y$, $z$; (iii) −0.5 + $x$, 1.5 − $y$, 2 − $z$; (iv) 1.5 − $x$, 0.5 + $y$, 2 − $z$; (v) −0.5 + $x$, 1.5 − $y$, −$z$; (vi) 0.5 + $x$, 1.5 − $y$, −$z$.

## Results and Discussion

**Descriptions of Crystal Structures.** The X-ray crystallographic analyses reveal that both **1** and **2** crystallize in the orthorhombic crystal system $P2_12_12$ and have a 3D framework. The asymmetrical unit contain one distinct M(II) ion, one D-cam ligand, half of TPOM ligand, and two guest water molecules (Figure S1, Supporting Information). As depicted in Figure 1a, the Zn(II) ion in **1** is four-coordinated by two pyridyl nitrogen atoms from two TPOM ligands and two oxygen atoms from two unidentate D-cam ligands, resulting in a slightly distorted $ZnN_2O_2$ tetrahedral geometry. The bond lengths [Zn−N = 2.064(4), 2.078(3) Å, Zn−O = 1.960(3), 1.942(3) Å, respectively] and angles [ranging from 97.2(1) to 129.6(2)°] around Zn(II) ions are within the normal ranges. Both carboxylate groups of the D-cam ligand in **1** monodentately coordinate to two adjacent tetrahedral Zn(II) ions. TPOM, on the other hand, has a distorted tetrahedral coordination geometry [N···C13···N angles ranging from 81.2(2) to 128.9(2)°], connecting four neighboring Zn(II) ions through its four peripheral pyridyl groups.

Compound **2** is isostructural to **1** but with a different coordination environment of the metal sites and a slightly larger unit cell. Because of the larger radius of Cd(II), both carboxylate groups in the D-cam ligand in **2** bidentately coordinate to two Cd(II) ions (Figure 1b). Cd(II) ion is six-coordinated by two pyridyl nitrogen atoms from two TPOM ligands and four oxygen atoms from two D-cam ligands. The Cd(II) center has a distorted octahedral coordination sphere [$CdN_2O_4$], being coordinated by two nitrogen atoms [Cd1−N1 = 2.281(5), Cd1−N2 = 2.332(5) Å], two oxygen atoms from one chelating carboxylate group [Cd1−O1 = 2.342(4), Cd1−O2 = 2.324(4) Å, O2−Cd1−O1 = 55.12(14) °], and two oxygen atoms from another bidentate carboxylate group [Cd1−O3 = 2.320(4), Cd1−O4 = 2.326(4) Å, O3−Cd1−O4 = 55.79(15)°]. This makes the Cd(II) ion a 4-connecting node, although it has octahedral coordination environment.

Both **1** and **2** possess a 4-connected 3D framework. It is interesting that even though both TPOM and the metal ions are tetrahedrally connected, the linkages between them do not form a 3D network and instead give rise to a 2D sheet. Tetrahedral TPOM ligand connects four M(II) ions through its four peripheral pyridyl groups, while each M(II) ion only connects two pyridyl nitrogens, with an N−M−N angle of 96.6(2)° (Zn) for **1** and 88.7(2)° (Cd) for **2**, respectively. This leads to the formation of a wavelike $[M_2(TPOM)]_n$ (M = Zn, Cd) 2D sheet with diamond-shaped pores (Figure 2). The 2D sheets stack over each other along the *c* axis, with a repeating distance of 8.780(1) Å in **1** and 9.760(1) Å in **2**, respectively. The bidentate D-cam ligands link two M(II) ions in neighboring sheets to form a 3D framework. It is interesting that such a connection between the D-cam and metal ions leads to an infinite helical 1D chain $[M(D\text{-cam})]_n$ running along the *a* axis (with a pitch of 14.373(2) Å for **1** and 13.275(1) Å for **2**, respectively) (Figure 3). All the helical chains are homochiral and exhibit the same left-handedness. In other words, the molecular chirality of D-$H_2$cam induces the absolute left-handed helical chains in both structures. The homochiral left-handed helical $[M(D\text{-cam})]_n$ chains interweave the 2D wavelike $[M_2(TPOM)]_n$ sheets via sharing the metal sites to form a 3D homochiral framework (Figure 4). Small square channels run along the *a* axis (the shortest distances between H atoms across the channel 4.19 × 5.12 $Å^2$ in **1**, 3.43 × 3.43 $Å^2$ in **2**, respectively). According to the previously proposed classification scheme for chiral materials,[6d] compounds **1** and **2** possess an $C_1A_2$ type structure (C and A represent chiral and achiral connectivity, whereas the subscript represents the dimensionality); that is, they are built on 1D homochiral chain connectivity and 2D achiral sheet connectivity.

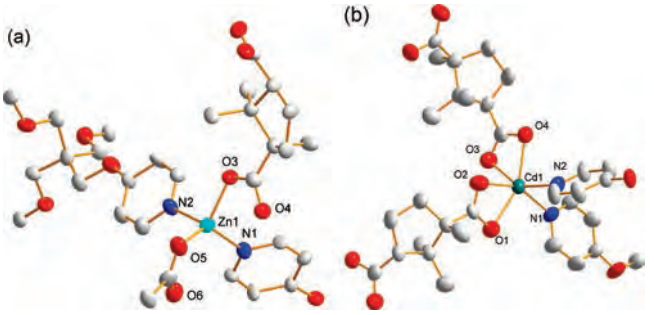


**Figure 1.** ORTEP drawings (with thermal ellipsoids at 50% probability) showing the coordination environment of the metal site in **1** (a) and **2** (b).

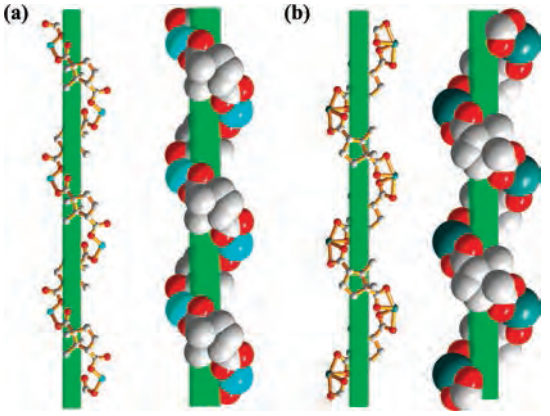


**Figure 3.** Perspective and space-filling views of the 1D left-handed helices of **1** (a) and **2** (b) along the *b* axis.

Better insight into the framework of **1** and **2** can be achieved by topology analysis. The tetradentate TPOM ligand can be considered as a regular tetrahedral T node and the M(II) center as another slightly distorted tetrahedral T node. All of the T nodes are 4-connected and the whole networks of **1** and **2** can be reduced into a 2-fold interpenetrating irregular α-quartz topology (Figure 5).[15] The short Schläfli symbol for the net is $6^48^2$, the long Schläfli symbol is $6.6.6_2.6_2.8_7.8_7$. The chiral quartz phase, being thermodynamically more stable than the diamond topology, exhibits unique piezoelectricity and thermally sensitive properties and is widely used in resonators and sensors.[16] However, only a few 3D homochiral porous MOFs with quartz topology have been successfully synthesized.[7f,17]

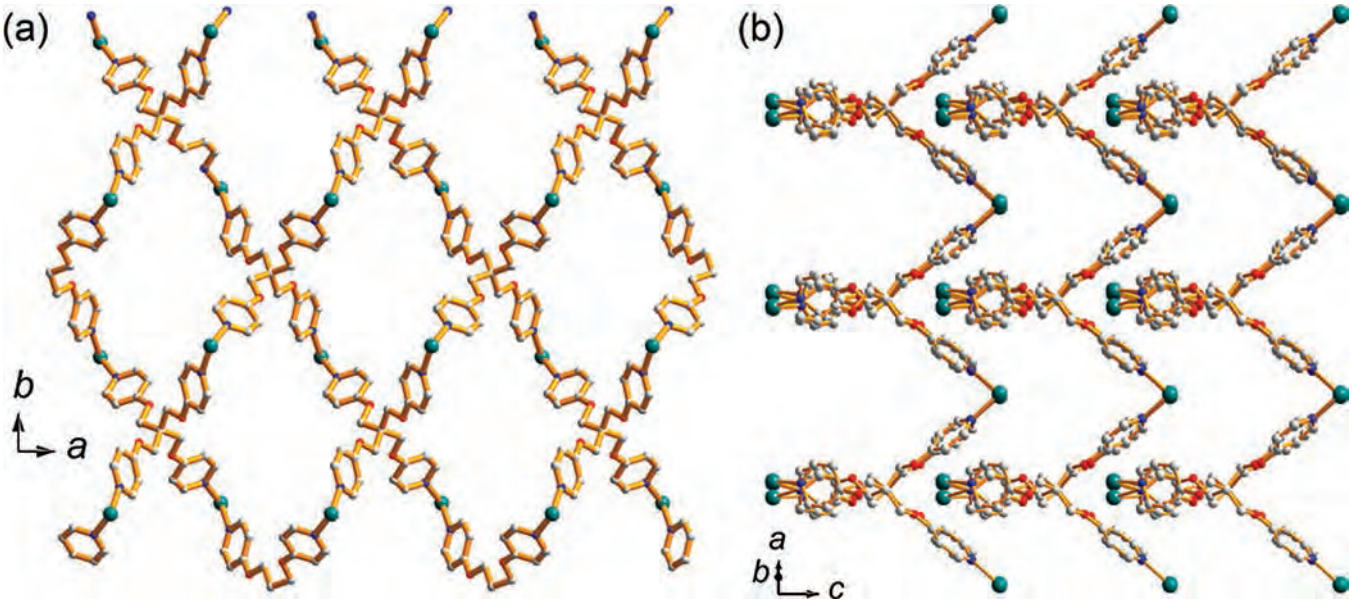


**Figure 2.** Perspective views of the wavelike 2D sheet built from tetrahedral TPOM ligands and M(II) ions along the (001) (a) and ($\bar{1}$20) (b) directions.

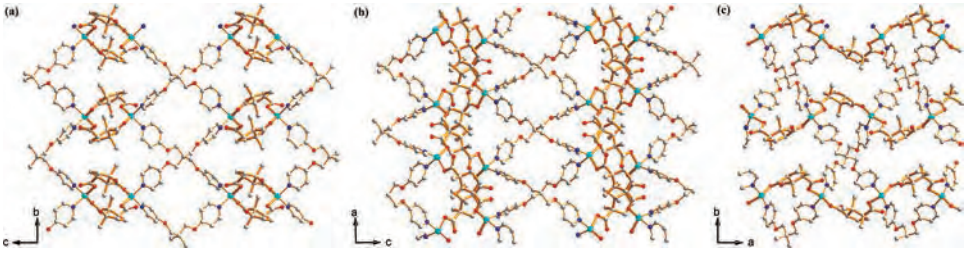

**Figure 4.** Perspective view of the 3D homochiral supramolecular network in **1** or **2** along the (a) *a*, (b) *b*, and (c) *c* axes.

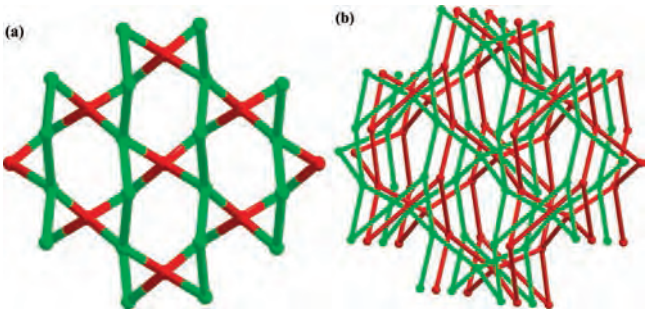


**Figure 5.** (a) A single $6^4 8^2$ net with different T nodes (M and TPOM) discriminated by colors. (b) 2-folded interpenetrating α-quartz network.

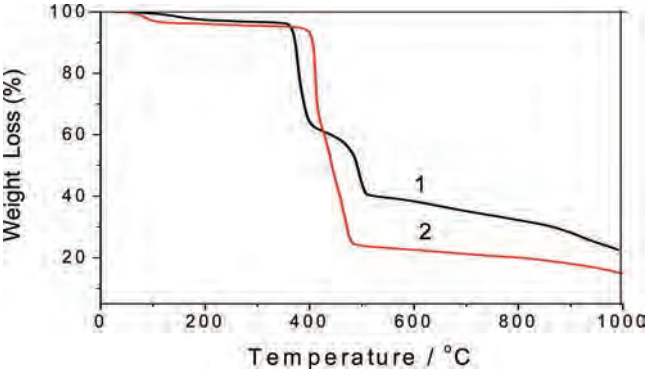


**Figure 6.** TGA curves for **1** and **2** under nitrogen.

Compounds **1** and **2** are the rare examples of MOFs that have an α-quartz topology with alternate metal ions and organic ligands as 4-connected T nodes. The interpenetration eliminates almost all the free space in **1** and **2**. The remaining free voids are partially filled with water molecules. Calculations using PLATON[18] based on the crystal structures show that the total solvent-accessible volume comprises 11.8% for **1** and 7.7% for **2**, respectively, of the total unit cell volume.

**Thermal Stability Analyses.** Thermogravimetric analyses (TGA) of **1** and **2** were conducted to determine their thermal stabilities, which are deemed an important property for MOFs.[19] For **1**, the TGA curve (Figure 6) shows the gradual weight loss of water molecules residing in the cavity (calculated 3.6%, observed 3.4%) in the temperature range of 110−185 °C. The host framework starts to decompose at ca. 370 °C. The weight loss of 38.3% between 370 and 390 °C corresponds to the decomposition of TPOM ligand (44.1% calculated). The third weight loss of 26.4% between 480 and 510 °C corresponds to the partial decomposition of D-cam ligands (39.3% calculated). This is followed by gradual loss of the residue at higher temperature. For **2**, the TGA curve shows the weight loss of water molecules (calculated 3.3%; observed 3.4%) in the temperature range of 60−100 °C. The host framework is stable up to ca. 407 °C. The weight loss rapidly occurs from 407 to 414 °C, corresponding to the loss of the TPOM ligand (40.3% calculated, 40.1% observed). When the temperature rises up, the D-cam ligand begins to decompose (31.2% at ca. 512 °C, 36.3% calculated). The remaining residue of 23.3 wt % at ca. 540 °C is consistent with the formation of CdO (23.3% calculated). The difference in thermal stabilities between **1** and **2** may be attributed to the small structural discrepancy in their coordination geometries.

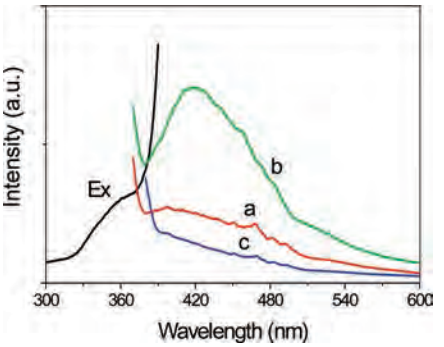


**Figure 7.** Photoluminescence spectra of **1** (a), **2** (b), and TPOM (c) in the solid state at room temperature.

The thermal stabilities of **1** and **2** were verified by PXRD analyses. PXRD patterns of the desolvented **1** and **2** match those of the pristine samples, suggesting their structures are intact after removal of solvent water molecules (Figure S2, Supporting Information). However, due to the limited pore opening, desolvented **1** and **2** exhibit no $N_2$ adsorption at 77 K. $H_2$ adsorption measurements show **1** and **2** adsorb 0.13 wt % and 0.09 wt % of $H_2$ under 1 atm and 77 K (Figure S3, Supporting Information), corresponding to 1.5 and 1.3 $H_2$ molecules per unit cell for **1** and **2**, respectively.

**Optical Properties.** Given that compounds **1** and **2** crystallize in a chiral space group ($P2_12_12$), their second NLO properties were studied. The quasi-Kurtz second harmonic generation (SHG) measurements were performed on powdery samples to evaluate their potential application as second-order NLO materials.[20] Before the SHG experiments, we check the phase purity of the bulk materials of **1** and **2** by PXRD and CD spectra. The experimental XRD patterns agreed well with the simulated ones generated on the basis of the single crystal structure analyses for **1** and **2** (Figure S2, Supporting Information), suggesting the products are of a pure phase. The solid-state circular dichroism (CD) spectra of **1** and **2** were recorded on bulk materials with a KBr pellet between 200 and 500 nm (Figure S3, Supporting Information). Both CD spectra of **1** and **2** exhibit an obvious

positive Cotton effect at the similar wavelengths, suggesting the entire bulk samples of **1** and **2** are the same handed conformation. The CD spectra confirm the enantiomerically pure nature of **1** and **2**. The SHG experimental results from the bulk materials indicate that both **1** and **2** are SHG active with responses of ca. 0.8 and 0.9 times that of urea (ca. 8 and 9 times that of KDP), respectively. This SHG efficiency is relatively strong compared to other related MOF materials.[21] As both **1** and **2** exhibit remarkable thermal stability and are insoluble in common polar and nonpolar solvents, they may be used for practical applications.

**Photoluminescence Properties.** Considering $d^{10}$ metal complexes usually exhibit excellent luminescent properties, the photoluminescent properties of **1** and **2** were investigated. The results show that only coordination polymer **2** exhibits intense emissions, while **1** shows no obvious emissions upon excitation at 360 nm. Broad photoluminescence emission bands with a maximum at 429 nm ($\lambda_{ex}$ = 360 nm) are observed for **2** (Figure 7). To understand the nature of the emission spectra, the luminescence properties of the free TPOM ligands and D-$H_2$cam ligands under the same experimental conditions were recorded for comparison. No obvious emissions were observed in both cases. The emission bands in **2** could originate from the TPOM ligand due to the chelation of the ligand to the metal center. This enhances the "rigidity" of the ligand and thus reduces the loss of energy through a radiationless pathway.[22] The difference in photoluminescence spectra of **1** and **2** may be attributed to the different coordination environments of the Zn(II) and Cd(II) ions.

## Conclusions

In conclusion, two new 3D homochiral metal-organic polymers $M_2(TPOM)(D\text{-}Cam)_2(H_2O)_2$ (M = Zn for **1**, Cd for **2**) have been synthesized successfully by using a tetrahedral quadridentate linker TPOM and a bidentate chiral ligand D-camphorate. **1** and **2** are isostructural even though Zn and Cd have a different coordination geometry. Both structures are constructed from tetrahedrally connected TPOM ligands and metal sites, in which homochiral left-handed helical chains $[M(D\text{-}cam)]_n$ interweave the wavelike 2D sheets $[M_2(TPOM)]_n$ into a 3D homochiral open framework with a 2-fold interpenetrating α-quartz topology. The chirality transfers from the D-$H_2$cam ligand to the whole 3D framework. Both samples are enantiomerically pure and exhibit high thermal stabilities. The preparations of **1** and **2** further exemplify a promising route to synthesize new four-connected homochiral 3D porous materials by using a tetrahedral linker and an auxiliary chiral ligand.

**Acknowledgment.** We are grateful for financial support from the National Basic Research Program (2006CB806104 and 2007CB925101), and the National Natural Science Foundation of China (50772046, 20931004, 20531040, and 20721002).

**Supporting Information Available:** Crystallographic information (cif) files, figures of asymmetric units, PXRD, CD spectra, $H_2$ adsorption isotherms of **1** and **2**. This material is available free of charge via the Internet at http://pubs.acs.org.

## References

(1) (a) Yu, J. H.; Xu, R. R. *J. Mater. Chem.* **2008**, *18*, 4021. (b) Sun, J.; Bonneau, C.; Cantín, Á.; Corma, A.; Díaz-Cabañas, M. J.; Moliner, M.; Zhang, D.; Li, M.; Zou, X. *Nature* **2009**, *458*, 1154.

(2) (a) Lippert, B. *Angew. Chem., Int. Ed.* **2006**, *45*, 2503. (b) Asanuma, H.; Liang, X. G.; Yoshida, T.; Yamazawa, A.; Komiyama, M. *Angew. Chem., Int. Ed.* **2000**, *39*, 1316. (c) Mamula, O.; Zelewsky, A. V.; Bark, T.; Bernardinelli, G. *Angew. Chem., Int. Ed.* **1999**, *38*, 2945.

(3) (a) Seo, J. S.; Whang, D.; Lee, H.; Jun, S. I.; Oh, J.; Jeon, Y. J.; Kim, K. *Nature* **2000**, *404*, 982. (b) Xiong, R. G.; You, X. Z.; Abrahams, B. F.; Xue, Z. L.; Che, C. M. *Angew. Chem., Int. Ed.* **2001**, *40*, 4422. (c) Bradshaw, D; Prior, T. J.; Cussen, E. J.; Claridge, J. B.; Rosseinsky, M. J. *J. Am. Chem. Soc.* **2004**, *126*, 6106. (d) Lee, S. J.; Hu, A. G.; Lin, W. B. *J. Am. Chem. Soc.* **2002**, *124*, 12948. (e) Vaidhyanathan, R.; Bradshaw, D.; Rebilly, J. N.; Barrio, J. P.; Gould, J. A.; Berry, N. G.; Rosseinsky, M, J. *Angew. Chem., Int. Ed.* **2006**, *45*, 6495.

(4) (a) Ockwig, N. W.; Yaghi, O. M. *Acc. Chem. Res.* **2005**, *38*, 176. (b) Kitagawa, S.; Norob, S.-I.; Nakamurab, T. *Chem. Commun.* **2006**, 701. (c) Moulton, B.; Zaworotko, M. J. *Chem. Rev.* **2001**, *101*, 1629. (d) Chen, X.-M.; Tong, M.-L. *Acc. Chem. Res.* **2007**, *40*, 162. (e) Fujita, M.; Tominaga, M.; Hori, A.; Therrien, B. *Acc. Chem. Res.* **2005**, *38*, 369.

(5) (a) Kesanli, B.; Lin, W. B. *Coord. Chem. Rev.* **2003**, *246*, 305. (b) Bradshaw, D.; Claridge, J. B.; Cussen, E. J.; Prior, T. J.; Rosseinsky, M. J. *Acc. Chem. Res.* **2005**, *38*, 273. (c) Guillou, N; Livage, C; Drillon, M; Férey, G. *Angew. Chem., Int. Ed.* **2003**, *42*, 5314.

(6) (a) Zhang, J.; Bu, X. H. *Chem. Commun.* **2008**, 444. (b) Thuéry, P. *Eur. J. Inorg. Chem.* **2006**, 3646. (c) Chen, S.; Zhang, J.; Bu, X. *Inorg. Chem.* **2008**, *47*, 5567. (d) Zhang, J.; Chen, S.; Valle, H.; Wong, M.; Austria, C.; Cruz, M.; Bu, X. *J. Am. Chem. Soc.* **2007**, *129*, 14168.

(7) (a) Rood, J. A.; Boggess, W. C.; Noll, B. C.; Henderson, K. W. *J. Am. Chem. Soc.* **2007**, *129*, 13675. (b) Zhang, J.; Chen, S.; Bu, X. *Angew. Chem., Int. Ed.* **2008**, *47*, 5434. (c) Ma, C.; Wang, Q.; Zhang, R. *Eur. J. Inorg. Chem.* **2008**, 1926. (d) Zhang, J.; Chen, S.; Zingiryan, A.; Bu, X. *J. Am. Chem. Soc.* **2008**, *130*, 17246. (e) Zhang, J.; Bu, X. *Chem. Commun.* **2009**, 206. (f) Zhang, J.; Chen, S.; Zingiryan, A.; Bu, X. *J. Am. Chem. Soc.* **2008**, *130*, 17246.

(8) (a) Zhang, J.; Liu, R.; Feng, P.; Bu, X. *Angew. Chem., Int. Ed.* **2007**, *46*, 8388. (b) Zhang, J.; Yao, Y. G.; Bu, X. H. *Chem. Mater.* **2007**, *19*, 5083. (c) Dybtsev, D. N.; Yutkin, M. P.; Peresypkina, E. V.; Virovets, A. V.; Serre, C.; Ferey, G.; Fedin, V. P. *Inorg. Chem.* **2007**, *46*, 6843. (d) Zeng, M, H.; Wang, B.; Wang, X. Y.; Zhang, W. X.; Chen, X. M.; Gao, S. *Inorg. Chem.* **2006**, *45*, 7069. (e) Zhang, J.; Bu, X. H. *Angew. Chem., Int. Ed.* **2007**, *46*, 6115. (f) Zhang, J.; Chew, E.; Chen, S.; Pham, J. T. H.; Bu, X. H. *Inorg. Chem.* **2008**, *47*, 3495. (g) Wang, L.; You, W.; Huang, W.; Wang, C.; You, X.-Z. *Inorg. Chem.* **2009**, *48*, 4295.

(9) (a) Liang, X. Q.; Zhou, X. H.; Chen, C.; Xiao, H. P.; Li, Y. Z.; Zuo, J. L.; You, X. Z. *Cryst. Growth Des.* **2009**, *9*, 1041. (b) Zhang, J.; Wu, T.; Feng, P. Y.; Bu, X. H. *Chem. Mater.* **2008**, *20*, 5457.

(10) Ren, S. B.; Zhou, L.; Zhang, J.; Li, Y. Z.; Du, H. B.; You, X. Z. *CrystEngComm* **2009**, *11*, 1834.

(11) Zhang, Q. C.; Bu, X. H.; Lin, Z; Wu, T.; Feng, P. Y. *Inorg. Chem.* **2008**, *47*, 9724.

(12) Yang, Z. H.; Wang, L. X.; Zhou, Z. H.; Zhou, Q. L.; Tang, C. C. *Tetrahedron: Asymmetry* **2001**, *12*, 1579.

(13) Sheldrick, G. M. *SHELXS-97, Program for X-ray Crystal Structure Solution*; University of Göttingen: Göttingen, Germany, 1997.

(14) Sheldrick, G. M. *SHELXL-97, Program for X-ray Crystal Structure Refinement*; University of Göttingen: Göttingen, Germany, 1997.

(15) (a) Blatov, V. A.; Shevchenko, A. P.; Serezhkin, V. N. *Acta Crystallogr.* **1995**, *A51*, 909. (b) Blatov, V. A.; Carlucci, L.; Ciani, G.; Proserpio, D. M. *CrystEngComm* **2004**, *6*, 377.

(16) Defregger, S.; Engel, G. F.; Krempl, P. W. *Phys. Rev. B* **1991**, *43*, 6733.

(17) (a) Sun, J.; Weng, L.; Zhou, Y.; Chen, J.; Chen, Z.; Liu, Z.; Zhao, D. *Angew. Chem., Int. Ed.* **2002**, *41*, 4471. (b) Hoskins, B. F.; Robson, R.; Scarlett, N. V. Y. *Angew. Chem., Int. Ed.* **1995**, *34*, 1203. (c) Hu, S.; Tong, M. L. *Dalton Trans.* **2005**, 1165. (d) Tynan, E.; Jensen, P.; Kelly, N. R.; Kruger, P. E.; Lees, A. C.; Moubaraki, B.; Murray, K. S. *Dalton Trans.* **2004**, 3440.

(18) Spek, A. L. *Acta Crystallogr., Sect. A* **1990**, *46*, C34.

(19) Cavka, J. H.; Jakobsen, S.; Olsbye, U.; Guillou, N.; Lamberti, C.; Bordiga, S.; Lillerud, K. P. *J. Am. Chem. Soc.* **2008**, *130*, 13850.

(20) (a) Kurtz, S. K. *J. Appl. Phys.* **1968**, *39*, 3798. (b) Ok, K. M; Chi, E. O; Halasyamani, P. S. *Chem. Soc. Rev.* **2006**, *35*, 710.

(21) (a) Anthony, S. P; Radhakrishnan, T. P. *Chem. Commun.* **2004**, 1058. (b) Koshima, H; Miyamoto, H; Yagi, I; Uosaki, K. *Cryst. Growth Des.* **2004**, *4*, 807. (c) Kwon, O. P; Jazbinsek, M; Yun, H; Seo, J. I; Kim, E. M; Lee, Y. S; Günter, P. *Cryst. Growth Des.* **2008**, *8*, 4. (d) Zhao, H.; Qu, Z.-R.; Ye, H.-Y.; Xiong, R.-G. *Chem. Soc. Rev.* **2008**, *37*, 84.

(22) Valeur, B. *Molecular Fluorescence: Principles and Applications*; Wiley-VCH: New York, 2001.